

Topological changes in a two-dimensional foam cluster

S.J. Cox^{1,a}, M.F. Vaz², and D. Weaire¹

¹ Physics Department, Trinity College, Dublin 2, Ireland

² Instituto de Ciência de Materiais e Superfícies and Departamento de Engenharia de Materiais, Instituto Superior Técnico, Av. Rovisco Pais, 1096 Lisboa Codex, Portugal

Received 18 October 2002 / Received in final form 19 March 2003 /

Published online: 21 May 2003 – © EDP Sciences / Società Italiana di Fisica / Springer-Verlag 2003

Abstract. Experiments on a small cluster of bubbles in a nominally two-dimensional foam show an instability in which a topological change forces one of the bubbles to be ejected to the outside of the cluster at a point where this is not predicted by a two-dimensional model of a foam. This is interpreted in terms of the energy of the initial and ejected states and of the finite liquid content of the experimental system. A description of the distribution of liquid in various experimental set-ups suggests that the exact response may depend critically upon the type of system used. This is demonstrated experimentally with reference to small clusters of bubbles undergoing a single topological change.

PACS. 82.70.Rr Aerosols and foams – 46.32.+x Static buckling and instability

1 Introduction

Before tackling a three-dimensional (3D) problem, one often tries first to find a two-dimensional (2D) model which shares some of the properties of the full system and is more amenable to analysis. This is particularly true in the field of foams [1]. While three-dimensional foams are more familiar from everyday experience, much can be learned from the two-dimensional soap froth. The froth is, like its three-dimensional counterpart, a minimal surface and it has both elastic and yielding properties when stressed. There are also analogies with many other physical systems, such as metallic grain growth and the territories of nesting birds [2]. For both the experimentalist and the theorist, the 2D froth is a much easier system with which to work. In particular, these 2D systems are currently enjoying something of a renaissance in the field of rheology [3,4].

The 2D foam is also an ideal system in which to study surface-tension-dominated instabilities. The usual analysis of most such instabilities relies on the approximation of two-dimensionality (depending on, among other things, the assumption that the distance between the two surfaces confining the system is small compared with a length-scale of the system such as the bubble diameter). The system is also assumed to be dry, *i.e.* having a low liquid fraction.

Recently, Weaire *et al.* [5,6] introduced a class of “flower” bubble clusters (see Fig. 1(a)), small groups of bubbles that were shown to have many interesting properties. The study of those properties is continued here,

introducing the experimental realization and subsequent analysis. Weaire *et al.* [5] describe a *buckling* instability, in which a 2D cluster of bubbles can show one of many different equilibrated structures for given topology and (fixed) bubble areas. The occurrence of this instability was confirmed by numerical simulations, and provides an interesting application of the Hessian eigenvalue facility of the Surface Evolver [7,8].

The cluster consists of a ring of n bubbles (petals) of area A surrounding a central bubble whose area A_c is varied. The cluster becomes unstable to buckling below a critical value of the central area given approximately by equation (2) of reference [5]

$$A_c^*/A \approx 0.041(n-6)^2. \quad (1)$$

Therefore, the buckling occurs only for clusters with more than 6 petals. At this point the pressure in the central bubble is equal to the pressure external to the cluster and the cluster becomes “floppy”. That is, it can exhibit any one of various modes of distortion, including those shown in Figure 1(b)-(e), without any variation in energy (equivalent to line-length in 2D).

In the next section we offer some further interpretation of the 2D buckling instability as background to the description of the topological instability that follows.

2 The buckling instability

At the critical point for buckling, each petal has two straight sides and two sides which are arcs of *the same*

^a e-mail: simon.cox@tcd.ie

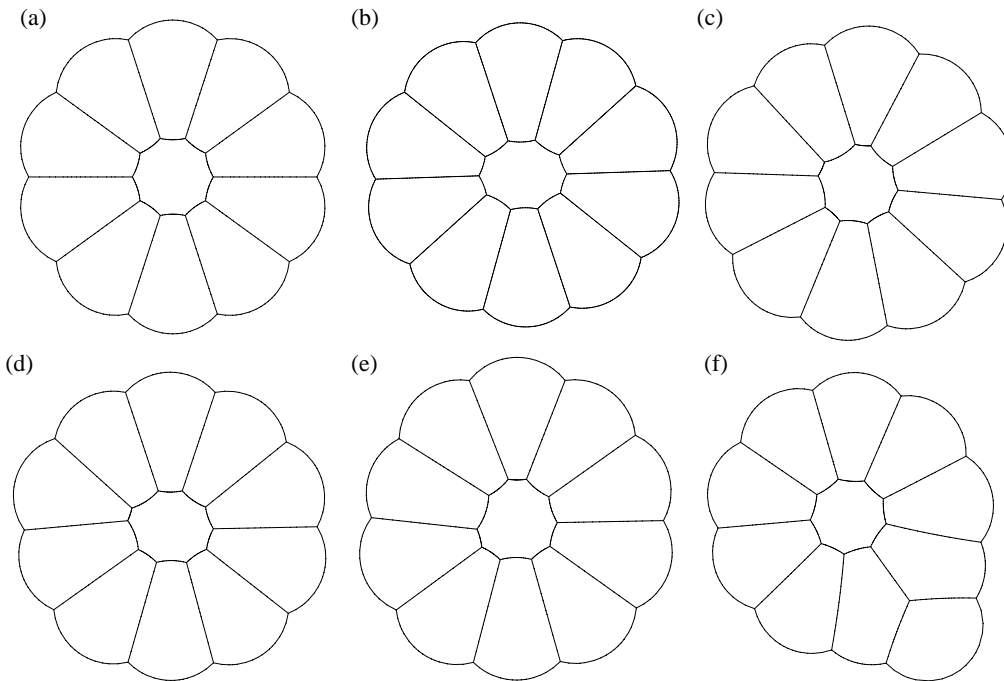


Fig. 1. Instabilities of 2D clusters. (a) A flower cluster consisting of a ring of $n = 10$ bubbles (petals) surrounding a central one. (b)-(e) Examples of buckled flower clusters; (b) is the case in which only the elliptical mode of distortion is present. In each case the energy of the configuration is identical. (f) A ten-petal cluster in which one bubble has been ejected after a single topological change.

circle [8,9]. The centre of each bubble is therefore well defined, so that we can idealize the cluster as a set of points connected by freely hinged rods of fixed length. In the case where all the petals are of equal size this corresponds to a regular polygon with n sides, but note that this constraint is no longer necessary, and the petals can have arbitrary areas. We now ask: how can this chain buckle while conserving the area inside it?

For fixed central area less than or equal to a critical value A_c^* , we now calculate the degrees of freedom. There are $2n$ vertex coordinates, less n constraints for the fixed rod-lengths, less three constraints for the possible translations or a rotation which we exclude. There just remains the area constraint. At the critical point itself, the fixed area of the central bubble is linearly dependent on the rod-lengths. This shows that there should be $n - 3$ modes of distortion, which correspond to the $n - 3$ decreasing eigenvalues found in Surface Evolver simulations [5]. For areas less than the critical one, there are therefore $n - 4$ modes that remain zero, and one increasing eigenvalue corresponding to the mode of distortion, shown in Figure 2.

When the area of the central bubble decreases below the critical area, the energy landscape therefore contains multiple, but energetically equal, minima. The modes of distortion correspond to the central bubble assuming a shape that relates to the possible modes of buckling of a freely hinged rod. For small numbers of petals, they will be elliptical modes; then as the number of petals increases, triangular modes of distortion are allowed, followed by square modes, etc. In general, the distortion will be com-

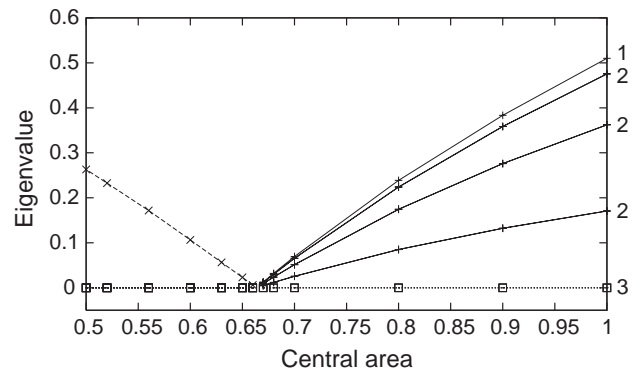


Fig. 2. The lowest ten Hessian eigenvalues for a cluster of $n = 10$ petals surrounding a central bubble whose area is decreased (cf. [5], Fig. 7). On the right are shown the multiplicities of each eigenvalue. Dotted lines denote zero values: of multiplicity three before buckling, and of multiplicity $n - 1$ afterwards. Solid lines show the $n - 3$ eigenvalues that descend to zero at the critical area, $A_c^* \approx 0.66$. The dashed line is the single eigenvalue which shows the distortion, in this case an elliptical one as shown in Figure 1(b).

posed of a combination of these modes, as illustrated in Figure 1(b)-(e) for a cluster with ten petals.

3 The ejection instability

The instability which we describe below concerns the change in topology which should occur when the

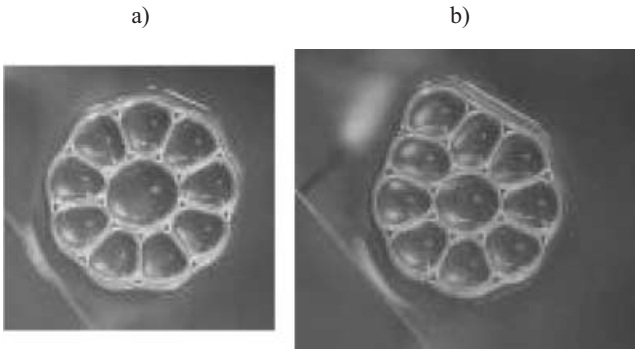


Fig. 3. Experimental observation of bubble ejection. (a) A stable cluster with $n = 9$ and $A_c/A = 2.49$. (b) Bubble ejection has occurred with $A_c^{**}/A = 2.25$. (See also Fig. 6 for the interpretation of these pictures.)

reduction in the area of the central bubble is pursued beyond the buckling instability.

In the idealized dry foam, one of the internal edges would shrink until its length is zero, initiating a T1 “neighbour-switching” transformation. This change in topology reduces the energy by ejecting a bubble to the outside of the cluster to give a configuration such as the one shown in Figure 1(f).

In studying a flower cluster experimentally, we are prevented from observing the buckling instability because it is pre-empted by this topological change. This ejection instability turns out to be of interest in its own right. We will argue that it is due to the finite liquid content and the three-dimensional nature of the experimental system.

We have performed experiments, described in Section 4, which give the critical area of the central bubble at which the ejection occurs. In Section 5 we calculate the value of central area at which the energy of the ejected state is lower than the symmetric one. It turns out that the experimental results lie precisely along this line, which we attribute to the influence of the underlying liquid in the type of 2D system used here (identical to that described in [10]). That is, the presence of the liquid allows the topological changes to occur when the relevant internal edges still have non-zero length.

Since the natural explanation of this is in terms of 3D effects, we describe the various experimental systems that have been used for the study of 2D foams in Section 6, and indicate the precise distribution of liquid in each of them. In future it may be necessary to carefully distinguish between them. Before concluding, we describe further experiments in Section 7 which show that the topological changes occur independently of the length-scale of the system.

4 Experiments

The experimental apparatus consists of a liquid reservoir containing water and a small amount of surfactant. A glass plate is held over the reservoir, leaving a gap of approximately $h = 3$ mm. A monodisperse cluster of n petal

bubbles is made by blowing air steadily through a capillary tube. We first isolate one of these bubbles, which is therefore circular, and measure its diameter d . We can then calculate the area of the petals, $A = \pi d^2/4$. The large central bubble is then created with a syringe. The cluster is adjusted, using the method described in [11], until the large bubble lies at the centre of the cluster, as shown in Figure 3(a). We then slowly reduce the area of the central bubble by sucking air from it through a syringe. The central bubble appears at all times to be roughly circular, so that its diameter is uniquely defined. We record this diameter d_c at frequent intervals until the ejection occurs, as in Figure 3(b). Using the last value of the diameter allows the calculation of the critical central area for ejection, $A_c^{**} = \pi(d_c)^2/4$.

Note that the central bubble is not exactly circular, cf. Figure 1(a). The difference in area between a circular bubble and one satisfying the 120° condition at vertices is less than 4% for n between 7 and 18. We expect that this is less than the experimental error.

We have found the critical central area for a range of values of the number of petals n . The results are shown in Figure 4 and are compared with the critical area at which the buckling occurs (1). The experimental results lie above the predicted central area for buckling.

This suggests that it should be possible to change between the ejected and symmetric states with only very small changes in central bubble area. As the liquid content in the experimental system decreases, however, the energy barrier is raised and the ejection is delayed until lower values of central area.

5 Energy of the ejected state

At each value of central bubble area the cluster seeks its minimum energy state. In a wet system, such as in the experiments described here, the effect of the liquid is to allow the system to avoid the energy barrier which separates alternative states in the strictly 2D model and to move to the ejected state at a larger value of central area than dry calculations would predict. Figure 5 shows this schematically for energy values of the 12-petal cluster. In the dry case, we would expect that as the central area is reduced, the cluster would first buckle and then eject a bubble (path $X B_d E_d^n Y$). However, the presence of liquid in the system means that the cluster ejects a bubble at E_w^n . Pursuing the reduction in central area further will, rather than allowing the cluster to buckle, show that another bubble will be ejected (E_w^{n-1}) before the point is reached at which the cluster with one ejected bubble might be expected to buckle.

By calculating the energy (line-length) of both the symmetric and the ejected structures, we are able to provide an upper limit to the central area at which (the first) ejection occurs. We shall find the largest value of central area at which the energy of the 2D cluster is lowered when a bubble is ejected. Comparison with the experimental results suggests that this limit is in fact the actual area at which ejection occurs, because our experimental system

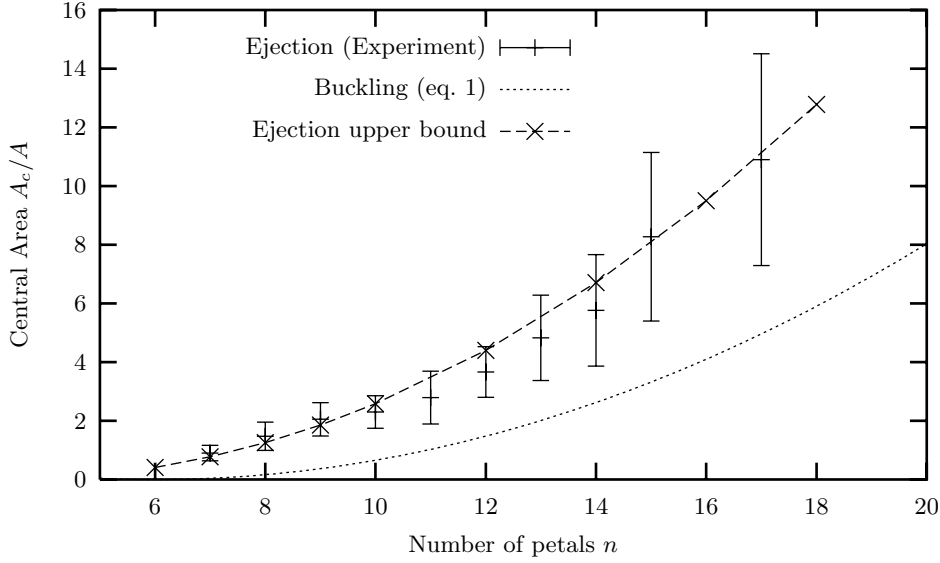


Fig. 4. The central area, normalized by the petal area, A_c/A , at which a bubble is ejected in an experiment in which this area is slowly decreased. Experimental data points are each averaged over three experiments and the standard deviation shown. The crosses show the largest central area at which an ejected configuration has lower energy; it can be fitted approximately by $A_c^{**} = 0.06(n - 3.45)^2 A$ which is shown as a dashed line. Also shown is the theoretical critical central area at which a flower cluster would buckle in a 2D theory of dry foam, equation (1).

contains enough liquid that it can slip to the ejected state as soon as it becomes energetically favourable.

The energy of the symmetrical cluster in 2D is given by

$$E_s = 2\sqrt{n} \left(\sqrt{(A_c + nA) \left(\frac{\sin \theta_+}{2 \sin(\pi/n)} + \theta_+ \right)} - \sqrt{A_c \left(\frac{\sin \theta_-}{2 \sin(\pi/n)} - \theta_- \right)} \right), \quad (2)$$

where $\theta_{\pm} = \pi/6 \pm \pi/n$ [12]. We are unable to calculate the energy of the ejected state analytically, but instead, for a range of values of n , compute it for several values of A_c , using the Surface Evolver in an efficient mode in which edges are treated as arcs of circles [7]. We then find the point at which these two energies are equal, shown in Figure 4. The data fit very well to a quadratic power law:

$$A_c^{**} = 0.0602(n - 3.45)^2 A, \quad (3)$$

representing the highest value of central area at which ejection may occur, showing close agreement with the experimental results.

These results suggest that a bubble could only be ejected from the ring whenever there are *more* than three petals in the cluster. This is reasonable, since with only three petals the ejection process would leave an unstable two-sided bubble that would undergo a further T1.

The proximity of the experimental data to this upper bound suggests that it should be experimentally possible to change between the ejected and symmetric states with only very small changes in central bubble area. Unfortunately, with our set-up we are only able to withdraw air

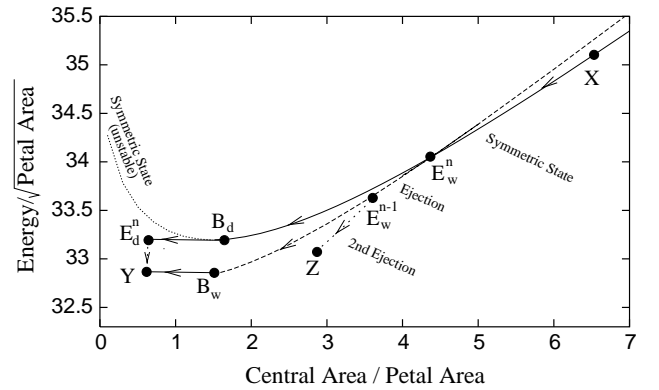


Fig. 5. The energy of a 2D flower cluster is shown in the case of $n = 12$ petals (surface tension is set equal to one). Consider an experiment in which the central area is progressively reduced from a high value. In the ideal 2D dry system, the cluster remains symmetric until it buckles at point B_d . At E_d^n (which depends upon the precise mode of buckling) an internal length shrinks to zero and the cluster undergoes a T1 change and ejects a bubble, following path $X B_d E_d^n Y$. The point Y represents an (unattainable) buckled cluster with one petal ejected. The presence of liquid in the real experimental system allows the cluster to cross the apparent energy barrier at or close to E_w^n and to eject a bubble. The $(n - 1)$ -sided central bubble might then be expected to buckle at point B_w , so that the wet cluster follows path $X E_w^n B_w Y$. However, the presence of liquid causes the ejection of a second bubble close to E_w^{n-1} . The cluster therefore progresses to point Z due to the further cascades of bubble ejection which will always pre-empt buckling.

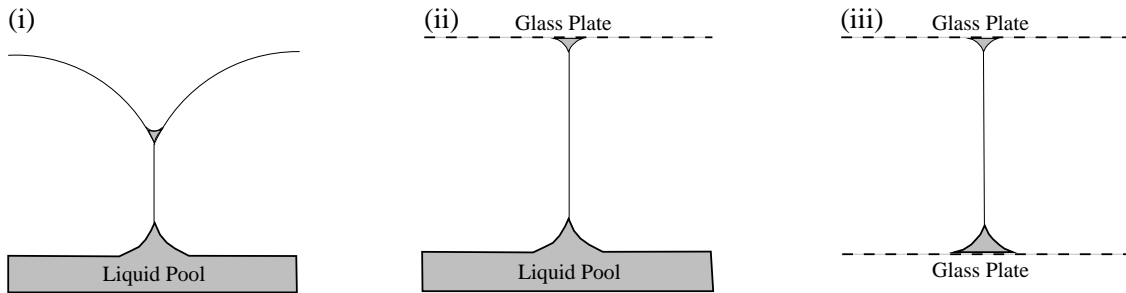


Fig. 6. Cross-sections through three distinct experimental systems which are used in experiments on nominally 2D soap froths: (i) Bragg bubble raft on a liquid pool; (ii) bubbles between a liquid pool and a glass plate; (iii) bubbles between two glass plates.

from the bubble, so are unable to test this hypothesis. As the liquid content in the experimental system decreases, however, the energy barrier is raised and the ejection is delayed until lower values of central area. We expect this to result in hysteresis as the central bubble area is alternately increased and decreased.

6 Two-dimensional froths: theory and experiment

Before describing the distribution of the liquid in the experimental system in detail, we must first review the prevailing theoretical and experimental models of 2D foams. It will become clear that the experimental set-up may play a significant role in determining the behaviour of the system.

The standard theoretical model of a *dry* 2D foam implies that it consists of arcs of circles which meet in threes at angles of 120° . For small numbers of bubbles, quantities such as the energy (line-length) and the bubble areas can be calculated analytically. However, these 2D configurations are relatively straightforward to obtain computationally: early examples of such code were written by Kermode and Weaire [13] and Herdtle and Aref [14]; recently the Surface Evolver [7] has been commonly used.

To simulate a *wet* 2D foam, one approach is to “decorate” each three-fold vertex with a small triangular Plateau border [15]. For the more general wet case, software written by Bolton and Weaire [16] was used to study rheological properties [17]. In this 2D point of view, a T1 process occurs when two neighbouring Plateau borders touch, *i.e.* when the length of the edge between them shrinks to zero. As the foam becomes wetter, the size of the Plateau borders increases and the edge length decreases, so that topological change is more likely to occur. However, a calculation of the necessary size of the Plateau borders shows that such a 2D model is insufficient to explain our experimental results. We must therefore seek a different explanation, which entails looking closely at 3D effects in the experimental system.

There are three standard experimental methods of producing so-called 2D bubble clusters, and it appears that their slight differences will cause different behaviour in precise studies of instabilities of foams of the kind dis-

cussed here. These experimental set-ups are illustrated in cross-section in Figure 6:

- (i) The Bragg bubble raft [18], in which a single layer of bubbles floats freely on a liquid surface.
- (ii) The system used here in which the bubbles are trapped between a glass plate and the liquid surface (*e.g.*, [10]). It is similar to the set-up perhaps first used by the author of [19], although he also used the following system.
- (iii) A layer of bubbles trapped between two glass plates [19, 20].

Where a soap film meets a glass plate there is a (surface) Plateau border running along the plate; these borders are smaller at the top plate due to the effect of gravity. Where a soap film meets the liquid pool there is a meniscus of height $l_c = \sqrt{2\gamma/\rho g}$, where γ is the surface tension and ρ the density of the liquid, and g is the acceleration due to gravity. (For our system (*i.e.* water and surfactant) the height of the meniscus, l_c , should be approximately 2.5 mm.) Both menisci and the surface Plateau borders meet in threes and join with a vertical Plateau border to give a fourfold vertex.

The principal difference between the usual realization of a 2D soap froth (case (iii)) and the other two may lie in the replacement of the lower Plateau border by a meniscus which is not of finite extent. Neighbouring menisci interact, as described by Nicolson [21] and by Shi and Argon [22] in their analysis of the Bragg raft, with a potential energy which decreases with separation. Such an analysis should be possible for the case of vertical Plateau borders on a liquid surface, and in future work we hope to explore this situation using three-dimensional simulations with the Surface Evolver.

7 Length-scale effects

In the meantime, however, we performed another series of measurements which allow us to make one further observation: the topological changes, caused by the attraction between neighbouring fourfold vertices via the meniscus, occur at a critical bubble area ratio which appears to be independent of the scale of the experimental system.

These experiments involved a cluster of only four bubbles of equal size. We varied both the separation h of the glass plate from the liquid surface and the volume $V = Ah$

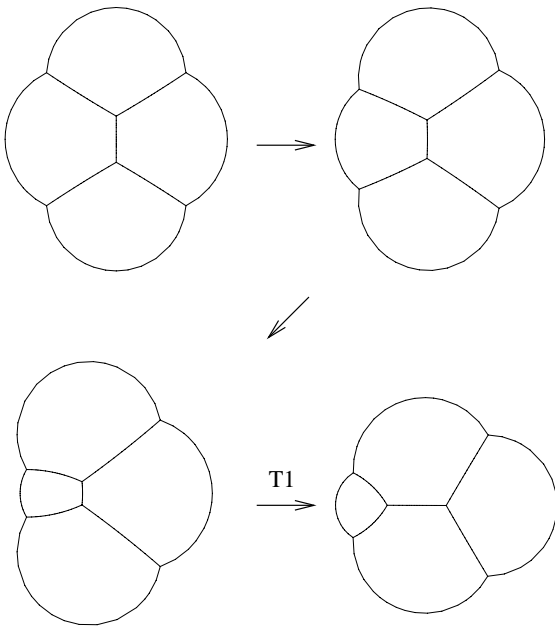


Fig. 7. To investigate the effect of the meniscus, we start with a cluster of four bubbles with equal volumes. The volume of one bubble is then slowly decreased until a topological change occurs. In the ideal dry limit, this T1 occurs only when the critical volume is vanishingly small, but our experiments show that it happens at a finite volume that depends upon the separation of the glass plate from the liquid in the experimental system.

of the bubbles. For each value of V and h we slowly reduced the volume of one of the four bubbles using the same techniques as above, until a T1 change occurred. This is shown schematically in Figure 7. In the dry limit, we should not expect the T1 to occur until the volume of the shrinking is vanishingly small, but the experiments on a wet system show that the critical area is finite.

This critical area of the shrinking bubble is recorded in Figure 8, showing data for values of h greater than the capillary height l_c (the behaviour for $h < l_c$ is markedly different due to the dominant effect of the meniscus). The critical area at which the T1 occurs is independent of the separation of the glass plate from the liquid surface, and depends linearly on the area of the large bubbles. We rationalize this by appeal to the following scaling argument, which shows that the elastic resistance of the soap films to allowing a T1 decreases with increasing cluster size.

Consider a cluster of fixed shape, with linear scale $L(\propto \sqrt{A})$, in which two vertices in the meniscus interact. We denote their initial separation by l , which is also proportional to L . We now perturb the system, reducing this separation by a distance Δl . To lowest order, Δl is determined by a balance between the attractive force F of the vertices, and the elastic resistance R of the soap films, which we express as the ratio $\Delta l = F/R$.

For all but the shortest distances, the attractive force F can be treated as a constant to lowest order. We approximate the elastic resistance by the second deriva-

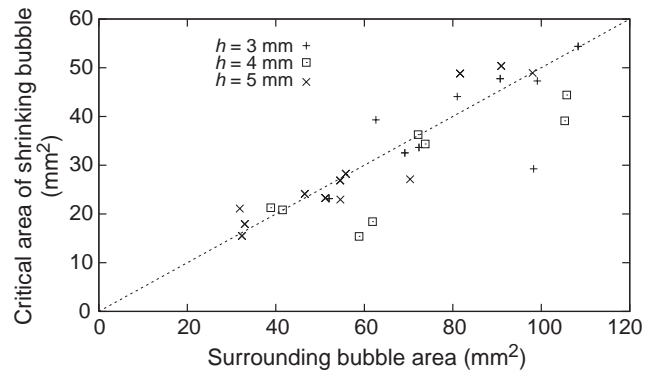


Fig. 8. The critical area of the shrinking bubble, described in Figure 7, at which a T1 topological change occurs in a cluster of four bubbles. The T1 occurs at a critical area of the shrinking bubble which is independent of the separation h . Moreover, the critical area depends linearly (the dashed line is a guide for the eye with slope one-half) on the area of the large bubbles. We show data only for values of h greater than the capillary height l_c , since the behaviour for $h < l_c$ is markedly different due to the dominant effect of the meniscus.

tive of the energy of the (dry) cluster with l , so that $R \sim L/L^2 = L^{-1}$. Then $\Delta l/l$ is constant.

The condition for a topological change is that Δl is approximately equal to l , so that a cluster that satisfies this condition will do so independently of the scale L .

8 Conclusions

While investigating experimentally the multiple states of two-dimensional foams, we have encountered an unexpected *ejection* instability. This is provoked by a topological (T1) change that moves the system to a lower energy state. The instability occurs before that predicted by a theory based upon dry foams: the presence of even a small amount of liquid in the experimental system provokes the T1 as soon as the energy of the ejected state is lower.

We chose one of the three possible experimental systems used for studying 2D froths, the case of a cluster sandwiched between a glass plate and a liquid surface. In describing the distribution of liquid in such a cluster, it becomes apparent that perhaps the three systems do not show the same response. In this case it appears to be the meniscus that causes the discrepancy. This may be a significant factor in the differences between the rheological results of Debregas *et al.* [3] and Lauridsen *et al.* [4] for example.

We are currently undertaking further work to elucidate and quantify further these effects, and identify more clearly than heretofore the essential differences between the three experimental systems of Figure 6. In particular, it now seems worthwhile to perform identical experiments on the systems shown in cases (ii) and (iii), with as little entrained liquid as possible, to ascertain the effect of the meniscus. While it seems likely that the Plateau borders that are present in the case of two glass plates would also engender a discrepancy from the dry case, this

effect should decrease to zero as the liquid content is decreased [16].

Together with other related investigations, such studies are needed to understand in fully quantitative terms the properties of real 2D foams. Whereas they were introduced by Smith [19] with qualitative effects and general topological properties in mind, today they are subject to much closer scrutiny. They seem to provide an excellent test bed for the development of models of the behaviour of soft matter, which may prove to be of much wider relevance.

The authors wish to thank F. Graner, W. Drenckhan and M.A. Fortes for useful discussions, and K. Brakke for unstinting assistance with the Surface Evolver. SJC thanks IST for hospitality, and SJC and DW acknowledge support from the European Space Agency and the Ulysses France-Ireland exchange scheme.

References

1. D. Weaire, S. Hutzler, *The Physics of Foams* (Clarendon Press, Oxford, 1999).
2. D. Weaire, N. Rivier, *Contemp. Phys.* **25**, 59 (1984).
3. G. Debregeas, H. Tabuteau, J.M. di Meglio, *Phys. Rev. Lett.* **87**, 178305 (2001).
4. J. Lauridsen, M. Twardos, M. Dennin, *Phys. Rev. Lett.* **89**, 098303 (2002).
5. D. Weaire, S.J. Cox, F. Graner, *Eur. Phys. J. E* **7**, 123 (2002).
6. S.J. Cox, D. Weaire, M.F. Vaz, *Eur. Phys. J. E* **7**, 311 (2002).
7. K. Brakke, *Exp. Math.* **1**, 141 (1992). Circular-arc mode is available with version 2.18d.
8. K.A. Brakke, F. Morgan, *Eur. Phys. J. E* **9**, 453 (2002).
9. B. Dollet, personal communication (2002).
10. M.F. Vaz, M.A. Fortes, *J. Phys. Condens. Matter* **9**, 8921 (1997).
11. M.F. Vaz, M.A. Fortes, *J. Phys. Condens. Matter* **13**, 1395 (2001).
12. F. Graner, personal communication (2001).
13. J.P. Kermode, D. Weaire, *Comput. Phys. Commun.* **60**, 75 (1990).
14. T. Herdtle, H. Aref, *J. Fluid Mech.* **241**, 233 (1992).
15. D. Weaire, *Philos. Mag. Lett.* **79**, 491 (1999).
16. F. Bolton, D. Weaire, *Philos. Mag. B* **65**, 473 (1992).
17. S. Hutzler, D. Weaire, F. Bolton *Philos. Mag. B* **71**, 277 (1995).
18. L. Bragg, J.F. Nye, *Proc. R. Soc. London, Ser. A* **190**, 474 (1947).
19. C.S. Smith, in *Metal Interfaces* (American Society for Metals, Cleveland, 1952) p. 65.
20. D.W. Thompson, *On Growth and Form*, 2nd edition (Cambridge University Press, Cambridge, 1942) p. 486.
21. M.M. Nicolson, *Proc. Cambridge Philos. Soc. Math. Phys. Sci.* **45**, 288 (1949).
22. L.T. Shi, A.S. Argon, *Philos. Mag. A* **46**, 255 (1982).